

Lossless polarization attraction simulation with a novel and simple counterpropagation algorithm for optical signals

M. Barozzi

Dip. Ing. Dell'informazione, Università degli Studi di Parma, viale delle Scienze 181/A, 43124-Parma, Italy

A. Vannucci

armando.vannucci@unipr.it

Dip. Ing. Dell'informazione, Università degli Studi di Parma, viale delle Scienze 181/A, 43124-Parma, Italy

D. Sperti

Nokia Siemens Networks, Rua dos Irmãos Siemens 1, 2720-093 Amadora, Portugal

We introduce a simple and fast iterative algorithm, named SCAOS (simple counterpropagation algorithm for optical signals), for simulating the counterpropagation of optical signals within a nonlinear fiber. Being based on the split-step Fourier method, the algorithm is easily implementable in many traditional optical simulators. Applications of the SCAOS algorithm to the vectorial nonlinear counterpropagation of a polarized pump and a probe signal demonstrate the phenomenon of lossless polarization attraction. The evolution of the signal polarization along the fiber, obtained by simulation, reveals that polarization attraction always entails a certain amount of degradation of the signal's degree of polarization. Two different setups are studied, involving different types of fibers with Kerr nonlinearity, and highlighting the dependence of the attraction phenomenon, as well as of its effectiveness, on the fiber type.

[DOI: <http://dx.doi.org/10.2971/jeos.2012.12042>]

Keywords: Nonlinear optics, polarization attraction, optical counterpropagation

1 INTRODUCTION

In many photonics applications, especially in optical fiber based systems, the state of polarization (SOP) of light remains so far an elusive uncontrolled variable, that can dramatically affect systems performance and that one would like to control as finely as possible. Recent experiments and simulations [1]–[4] have demonstrated that a lossless polarization attractor can be realized, even using telecom fibers at moderate signal powers [2]. The principle of operation of such a device, that is schematically depicted in Figure 1(b), is based on the injection of a counterpropagating fully polarized continuous-wave (CW) pump, whose SOP *attracts* any input probe signal SOP towards the same output polarization. As an example, Figure 1 (a and c) report, on the Poincaré sphere, an ensemble of 50 random (uniformly distributed) input probe SOPs and their corresponding output SOPs, as obtained from the system described in Section 4. The output probe signal SOPs clearly surround the pump SOP (blue, in Figure 1(c)), set by the polarization controller (PC, in Figure 1(b)) on S_1 , in this example. It is worth noting that, as opposed to other devices that employ polarization dependent loss/gain, as, e.g., those based on the Raman amplification [5, 6], the physical mechanism behind the lossless polarization attractor is merely the Kerr effect [3]. Repolarizing an arbitrarily (un-)polarized optical signal by means of a lossless instantaneous nonlinear interaction is a fundamental effect of great interest for telecommunication applications and optical signal processing systems. Rather than discussing possible applications, we concentrate here on the numerical simulation techniques for this phenomenon, which

entails counterpropagating signals as a fundamental prerequisite for the lossless attraction to happen [1].

Simulating polarization attraction requires the joint integration of the two vectorial nonlinear Schrödinger equations (VNLSE) of the pump and probe fields. Since the fields initial values are supplied at opposite fiber ends, the problem at hand is a Boundary Value Problem (BVP), that cannot be tackled with the split-step Fourier method (SSFM). Resorting to traditional finite difference integration requires large amounts of memory and long computation times: the authors of [1, 2] perform numerical simulations in the case of a short fiber (2 m) [1], leaving to experiments the case of long fibers (kilometers) [2].

The effects described in this paper are the same as those seen by other authors [2]–[4]. Hence, as we stress, there isn't any new physics, here. In this work, we describe a novel iterative algorithm for the numerical simulation of counterpropagating optical signals [7], which is based on the SSFM, hence can be implemented in many traditional optical simulators that were originally devised for copropagating channels. In addition, having the SSFM as the fast and efficient core of the algorithm's iterations makes it suitable for simulating counterpropagation even in (kms) long fibers [2], where finite difference integration is not practical. The proposed algorithm, named SCAOS (simple counterpropagation algorithm for optical signals), is then applied to simulate the nonlinear polarization interaction between a probe and a pump signals, that

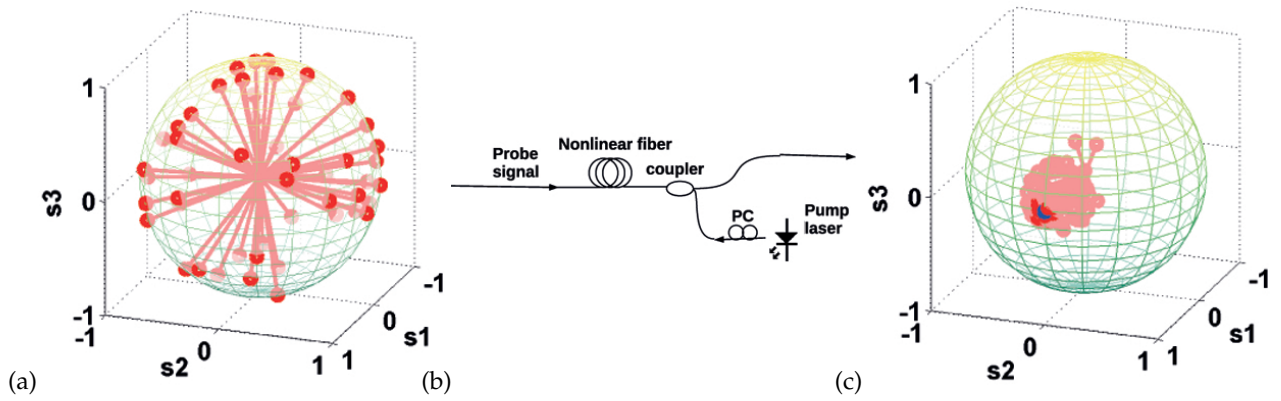


FIG. 1 (a) 50 random (uniformly distributed) input probe SOPs; (b) schematic setup of a lossless polarization attractor (polarization controller, PC, sets the pump SOP) ; (c) output average probe SOPs (DOP=magnitude), attracted towards the pump SOP (blue, here set on S_1).

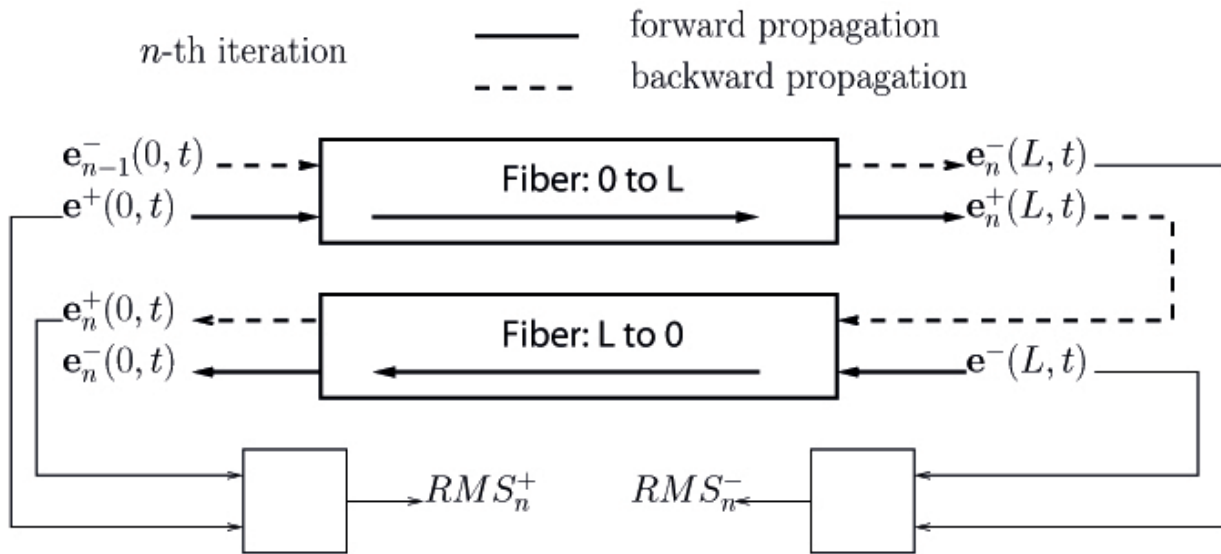


FIG. 2 Schematic description of the iterative SCAOS algorithm.

propagate in opposite directions, thus demonstrating the operation of a lossless Kerr-based polarization attractor.

2 THE SCAOS ALGORITHM

We wish to simulate the counterpropagation of a probe $\mathbf{e}^+(z,t)$ and a pump signal $\mathbf{e}^-(z,t)$, travelling within a fiber of length L , whose initial values $\mathbf{e}^+(0,t)$ and $\mathbf{e}^-(L,t)$ are given. Signal superscripts \pm identify the propagation direction, so that $\mathbf{e}^+(t)$ propagates from $z = 0$ to $z = L$, and vice-versa for $\mathbf{e}^-(t)$. Hence, the final result is to calculate the outgoing probe $\mathbf{e}^+(L,t)$ and pump $\mathbf{e}^-(0,t)$. The basic idea behind the proposed algorithm is to let \mathbf{e}^+ and \mathbf{e}^- iteratively propagate from $z = 0$ to $z = L$ and vice-versa (i.e., in the “reverse fiber”, as seen from $z = L$ to $z = 0$). In each propagation, one of the fields forward-propagates, starting from its given initial value, towards its output fiber end, while the other backward-propagates, i.e., travels according to an inverse-Schroedinger equation, starting from an estimated value. Backward-propagation is an option that can be easily implemented in the SSFM, which is originally devised for a fast and efficient (forward) signal propagation. We did so, while implementing the whole SCAOS algorithm, within

Optilux [8], the SSFM-based, open-source optical simulator developed at the University of Parma.

Figure 2 sketches the $n - th$ algorithmic iteration. Before the first iteration, the initial pump estimate $\mathbf{e}_0^-(0,t)$ is found by letting the pump initial condition $\mathbf{e}^-(L,t)$ forward-propagate as a single field, from L to 0 . After each half-iteration, the backward-propagating signal completes a round-trip towards its input fiber end, yielding a new $n - th$ estimate for the input field ($\mathbf{e}_n^-(L,t)$, at $z = L$, or $\mathbf{e}_n^+(0,t)$, at $z = 0$). A normalized root mean square (rms) error is calculated, between such an estimate and its true initial value. At the same time, the given initial (boundary) value is substituted to the estimate, so that the outgoing forward-propagating field ($\mathbf{e}_n^+(L,t)$, at $z = L$, or $\mathbf{e}_n^-(0,t)$, at $z = 0$, which are the sought quantities) is refined, at the next iteration.

The rms errors RMS_n^\pm , evaluated for the pump and probe at $n - th$ iteration, drive the stop criterion: the algorithm stops when both RMS_n^\pm are below a certain threshold, meaning that the round-trip field estimates are sufficiently close to their true initial values. Figure 3(a), obtained for the polarization attraction setup of Section 3, shows a typical behavior of the normalized rms errors, where the errors becomes negligible (below 0.1 %) in a few iterations.

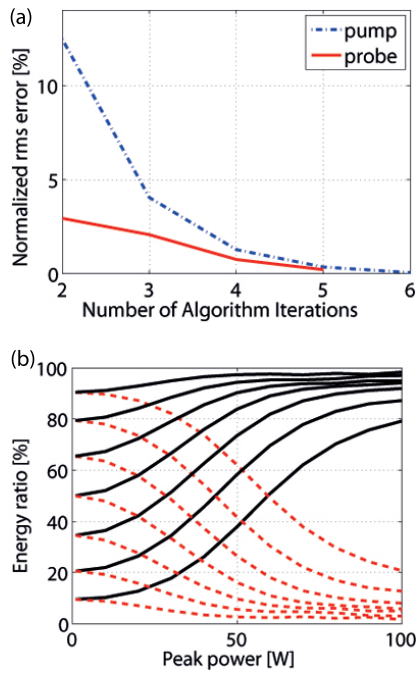


FIG. 3 (a) Residual normalized rms error during SCAOS iterations; (b) Fraction of probe energy that is attracted towards (solid line) a right-circular pump SOP, in a short lossless attractor, as in [1]. The residual fraction of probe energy, i.e., the energy of the probe component that is orthogonal to the attracting pump SOP, is plotted with dashed lines.

3 APPLICATION TO LOSSLESS POLARIZATION ATTRACTION IN A SHORT HIGHLY NONLINEAR FIBER

As a first application of the SCAOS algorithm, we simulate the system setup described in [1] and used for the first experimental demonstration of lossless polarization attraction. The counterpropagating pump and probe beams, both consisting of a completely polarized 10 ns intensity-modulated light pulse, are transmitted on a highly nonlinear single mode fiber, with length $L = 2$ m. The large Kerr coefficient ($\gamma = 22 \text{ W}^{-1}\text{Km}^{-1}$) and pulse intensities (up to 45 W) used in the experiments allow a significant nonlinear interaction. In such a short fiber, propagation is governed by the VNLSE, where circular polarizations play a special role, hence a right circular polarization is chosen for the input pump SOP (S_3 in Stokes space).

After propagating 7 different input probe SOPs with increasing ellipticity and random azimuth, Figure 3 shows the fraction of output probe energy that is aligned with (solid line) or orthogonal to (dashed line) the input pump SOP, as a function of the equal pump and probe peak powers injected into the fiber. Results coincide exactly with those reported in [1] (obtained with finite difference integration), and show how, as power increases, each input probe SOP is attracted towards the right circular polarization imposed by the pump.

To gain further insight into the polarization attraction process, we report in Figure 4 details about the polarization states of the pump and probe along the fiber, in the case of an input probe with linear horizontal SOP and input powers 100 W. The degree of polarization (DOP) of the launched pump and

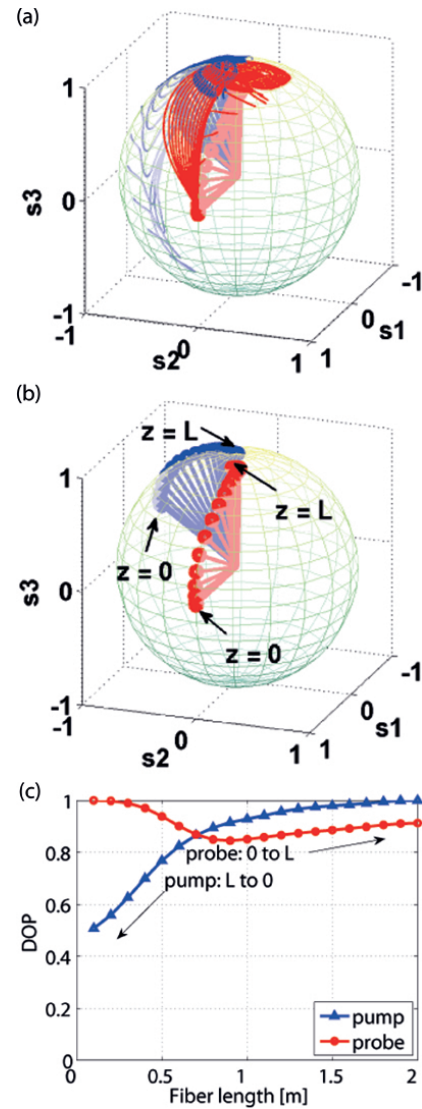


FIG. 4 Lossless polarization attraction between pulses in a short (2 m) highly nonlinear fiber: (a) SOP traces along z (red: probe, blue: pump) (animated GIF, 277 kB, available online); (b) motion of the average attracted SOP; (c) resulting DOP, along z .

probe pulses is unitary. This is no longer true when the two signal beams start interacting: Figure 4(a) shows the depolarization traces, for the probe (red) and pump (blue), on the Poincaré sphere. Each trace represents the time evolution of the pulse's SOP, at a given position $z \in [0, L]$ along the fiber, and the inner vectors represent its power-averaged SOP. From each trace, we report, in Figure 4(b,c), the average SOP and the DOP. The probe average SOP is attracted towards the pump SOP, with a relatively small depolarization, while the pump is much more depolarized and ends away from the input probe. Full results, as in Figure 4(a-c), are obtained with the SCAOS algorithm in 8 min. computation time, on an ordinary PC.

Different choices for the input probe SOP yield similar results: Figure 5(a) shows the resulting average output probe polarizations (marked by red vectors), obtained by simulation (through the proposed algorithm), when the attracting pump SOP (marked by a blue vector) is right circular (S_3). Results were obtained by launching 50 random input probe SOPs, with uniform distribution over the Poincaré sphere, as in Figure 1(a). As usual, polarization attraction entails a certain amount of depolarization: the DOP of the resulting out-

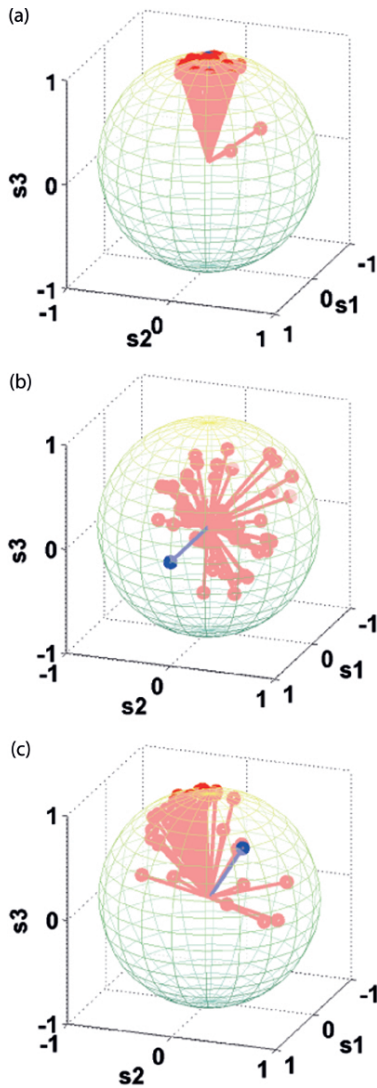


FIG. 5 Average probe SOP (red), at the output of a short (2 m) lossless polarization attractor (DOP=magnitude). Plots obtained for 50 random input SOPs, in the case of a circular (a), linear (b), and elliptical (c) pump SOP (blue).

put pulses is represented by the (red) vectors' magnitude, in Figure 5. Figure 5(a) shows an effective polarization attraction towards the right-circular pump SOP, for all but those probe SOPs that were initially almost orthogonal to the pump: as we verified, those are the input SOPs that are less attracted, on average, and whose output DOP is the lowest.

On the contrary, polarization attraction is not equally effective, in this setup, if the pump is not circularly polarized, as can be verified in Figure 5(b,c), obtained for a linear horizontal (b) or elliptically polarized (c) pump SOP. To quantify these results, we averaged the output probe SOPs in the figure and computed the magnitude of such an average¹, to get 0.81, 0.25, and 0.60, respectively. The result obtained for a left-circular pump, not reported in figures, was the same as that for the right-circular pump case in Figure 5(a). Hence, an effective polarization attraction occurs only in the case of a circularly polarized pump, while in the tested linear and ellipti-

cal pump cases (b,c) the attraction is much weaker: a fact that has not been sufficiently pointed out in [1].

As a further comment on the results in Figure 5(b,c), the detailed studies in [9, 10] pointed out that, in fibers where the VNLS holds, polarization attraction occurs towards a SOP that has the same ellipticity as the pump but an azimuth rotated by 180°, with respect to the pump². In [9, 10], attraction is studied as an asymptotical condition, for CW signals and in the limit of an infinitely long fiber. However, our results evidence that, for a fiber with finite length, as the one that we employed in the tested setup, the attraction condition is approached to a different extent, depending on the pump SOP, and is way more effective when a circularly polarized pump is injected.

4 APPLICATION TO LOSSLESS POLARIZATION ATTRACTION IN A LONG TELECOM FIBER

As demonstrated in [2], polarization attraction can happen even at moderate power levels, provided that the nonlinear polarization interaction occurs in a longer fiber. The second system setup to which we apply the SCAOS algorithm is similar to the one used for the experiments in [2]. An intensity modulated probe pulse, with duration 3 μs and peak power 1.2 W, undergoes lossless Kerr interaction with a counter-propagating CW pump, with equal power, on an ordinary telecom fiber, with Kerr coefficient $\gamma = 1.99 \text{ W}^{-1}\text{Km}^{-1}$ and length $L = 10 \text{ km}$. Thanks to the random birefringence of the fiber, propagation is governed by the Manakov equation [3, 4], where the Kerr effect is isotropic, on the Poincaré sphere. Hence, any pump SOP is expected to attract the probe SOP in the same way.

We thus chose, without loss of generality, a linear horizontal pump SOP (S_1), and obtained the simulation results shown in Figure 6, plotted in the same framework as those reported in Figure 4. Results refer to a right-circular input probe SOP, here chosen as an example, that yields the depolarization traces reported in Figure 6(a) (10 traces, plotted every km of propagation). The probe average SOPs, plotted on a finer scale in Figure 6(b), show that attraction occurs towards the pump SOP, along a spiral trajectory. The probe depolarization is visible in the DOP curve in Figure 6(c), while the pump depolarization is negligible here, being the pump much longer than the probe duration.

Repeating the propagation for 50 random input probe SOPs, i.e., those in Figure 1(a), yields similar results, as visible in Figure 7(b) (which is the same as Figure 1(c)), reporting the corresponding average output probe SOPs. Polarization attraction is testified by the 50 vectors surrounding the attracting pump SOP (S_1), and the output DOPs are reported as the vectors' magnitude. Figures 7(a),(c) complete the picture, by verifying numerically that a different choice of the pump SOP does not change the attractor's performance, at the output. Thanks to the isotropy of the Kerr effect, in the context of the Manakov

¹Such an averaging process, including both the temporal average, for each launched SOP, and an ensemble average, over the 50 launched SOPs, is the same as that adopted in [4, eq.(12)].

²Of course, the azimuth is undetermined when the pump SOP is circular (S_3), hence the circular pump case appears to follow the same "rule".

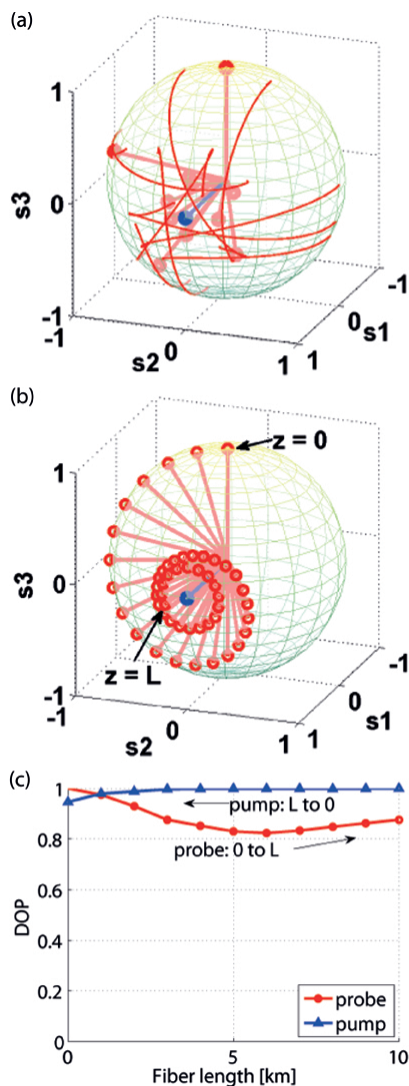


FIG. 6 Lossless polarization attraction of a probe pulse towards a (linear horizontal) CW pump, in a long (10 km) fiber. (a) probe SOP traces along z (animated GIF, 147 kB, available online); (b) motion of the average probe SOP (red) along z , showing the attraction towards the (blue) pump SOP; (c) resulting DOP, along z .

equation, and contrary to the case of a short highly-nonlinear fiber discussed in Section 3, all pump polarizations are equally effective in attracting the input probe SOPs. The overall performance, as quantified by the magnitude of the average output probe SOPs, as in Section 3, is equal 0.80, 0.76, and 0.78, respectively, for the tested right-circular, linear horizontal, and elliptical pump SOPs reported in Figure 7(a-c).

5 CONCLUSIONS

We introduced a novel iterative algorithm, named SCAOS, to simulate the counterpropagation of optical signals, and implemented it in the Optilux simulator [8]. We applied SCAOS to simulate the nonlinear polarization interaction between a pump and a probe field, due to Kerr effect. Two system setups were analyzed, showing that polarization attraction takes place both in a short highly nonlinear fiber, where powerful signals are launched, and in a long telecom fiber, even with moderate signal powers. We thus describe the same effects presented in recent literature [2]–[4], using an alternative numerical approach and obtaining consistent results. The al-

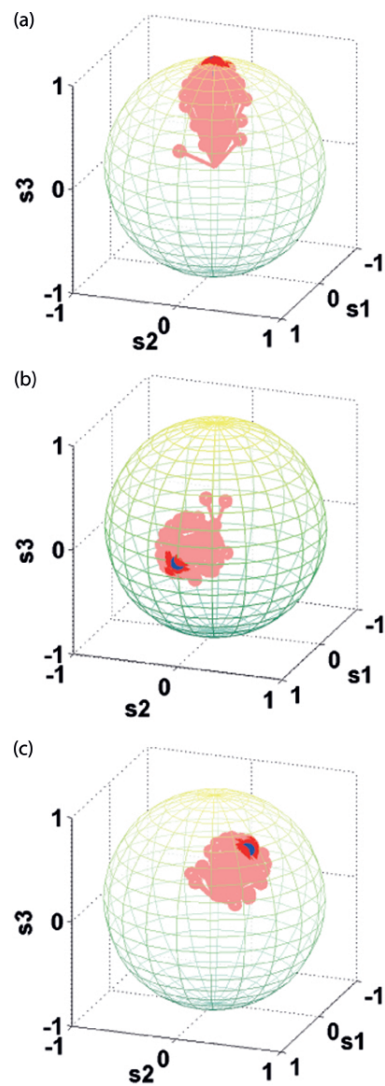


FIG. 7 Average probe SOP (red), at the output of a long (10 km) lossless polarization attractor (DOP=magnitude). Plots obtained for 50 random input SOPs, in the case of a circular (a), linear (b), and elliptical (c) pump SOP (blue).

gorithm, always converging in a few iterations (with fast computation times), allowed a detailed study of the signals’ polarization evolution, thus pointing out the dynamics of lossless polarization attraction. Results reveal that, while in the first case (short highly nonlinear fiber) the attracting pump should be circularly polarized, in the second case (long telecom fiber) an effective lossless polarization attraction occurs towards any pump polarization.

6 ACKNOWLEDGEMENTS

This work was performed within the PRIN 2008 project “Non-linear cross-polarization interactions in photonic devices and systems (POLARIZON)”, financially supported by the Italian Ministry for Education and Scientific Research (MIUR).

References

[1] S. Pitois, J. Fatome, and G. Millot, “Polarization attraction using counterpropagating waves in optical fiber at telecommunication wavelengths,” *Opt. Express* 16, 6646–6651 (2008).

- [2] J. Fatome, S. Pitois, P. Morin, and G. Millot, "Observation of Light-by-Light Polarization Control and Stabilization in optical Fibre for Telecommunication Applications," *Opt. Express* **18**, 15311–15317 (2010).
- [3] V. Kozlov, J. Nuño, and S. Wabnitz, "Theory of lossless polarization attraction in telecommunication fibers," *J. Opt. Soc. Am. B* **28**, 100–108 (2011).
- [4] V. Kozlov, J. Fatome, P. Morin, S. Pitois, G. Millot, and S. Wabnitz, "Nonlinear repolarization dynamics in optical fibers: transient polarization attraction," *J. Opt. Soc. Am. B* **28**, 1782–1791 (2011).
- [5] P. Martelli, M. Cirigliano, M. Ferrario, L. Marazzi, and M. Martinelli, "Attrazione di polarizzazione indotta da amplificazione raman," in *Proceedings to Fotonica 2009, 11° Convegno Nazionale delle Tecnologie Fotoniche*, B4.3 (AEIT, Pisa, 2009).
- [6] F. Chiarello, L. Ursini, L. Palmieri, and M. Santagiustina, "Polarization Attraction in Counterpropagating Fiber Raman Amplifiers," *IEEE Photonic. Tech. L.* **23**, 1457–1459 (2011).
- [7] M. Barozzi, A. Vannucci, and D. Sperti, "A simple counter-propagation algorithm for optical signals (SCAOS) to simulate polarization attraction," in *Proceedings to Fotonica 2012, 14° Convegno Nazionale delle Tecnologie Fotoniche*, A6.4 (AEIT, Firenze, 2012).
- [8] P. Serena, M. Bertolini, A. Vannucci, "Optilux Toolbox," available at http://optilux.sourceforge.net/Documentation/optilux_doc.pdf.
- [9] S. Lagrange, D. Sugny, A. Picozzi, and H. R. Jauslin, "Singular tori as attractors of four-wave-interaction systems," *Phys. Rev. E* **81**, 016202 (2010).
- [10] E. Assémat, S. Lagrange, A. Picozzi, H. R. Jauslin, and D. Sugny, "Complete nonlinear polarization control in an optical fiber system," *Opt. Lett.* **35**, 2025–2027 (2010).